Challenges in LoS Terahertz MIMO

Suresh Singh
Department of Computer Science
Portland State University
Portland, Oregon 97207
Email: singh@cs.pdx.edu

Ha Tran
Department of ECE
Portland State University
Portland, Oregon 97207
Email: tranha@pdx.edu

Thanh Le
Department of ECE
Portland State University
Portland, Oregon 97207
Email: thanh4@pdx.edu

Abstract—This paper examines a 2x2 LoS (Line of Sight) MIMO (Multiple Input Multiple Output) channel for terahertz communications. Utilizing measurements, we extract channel models which are then used in a simulation to produce bit error rate curves for uncoded QPSK (Quadrature Phase Shift Keying). The specific focus of this work is on studying the impact of changing transmitter receiver distances and relative orientation. Since the terahertz band has a small wavelength, such small movements can have a large impact on the channel. The results support this intuition and show that horizontal displacements of one antenna relative to another by distances as small as 1-2 cm can cause the bit error rate to increase by an order of magnitude. Similarly, utilizing sub-optimal antenna spacing at the transmitter and receiver can also result in similar types of performance degradation. This study illustrates that while LoS MIMO is an effective approach for utilizing the large terahertz bandwidth, we need to consider the effects of antenna deployments.

Index Terms—Terahertz, channel model, propagation, MIMO

I. INTRODUCTION

The terahertz band (from 0.1 to 10 THz) is emerging as the next segment of the radio spectrum to be explored for communications. Terahertz is mostly used today for sensing applications, such as detection of various chemicals or for scanning the body for skin cancer or at the airports (the full body scanner), and other similar applications [1], [2]. However, various research groups have been studying the potential of utilizing this spectrum for communications [3]–[5]. The reason for this interest is the ability to provide very high-bandwidth channels [6], [7] over short distances [8], [9]. This can enable a quantum leap in the types of applications that can be deployed.

MIMO (Multiple Input Multiple Output) is an appropriate mechanism to deliver high data rates at these frequencies. Given the small wavelength, these arrays can be made small. However, this part of the spectrum suffers significant attenuation in the atmosphere and reflections are virtually undetectable, see Figure 1. As a result, we need to consider LoS (Line of Sight) MIMO channels rather than the more common NLoS channels studied at lower frequency bands. Unfortunately, LoS channel capacity can be greatly affected by simple changes in transmitter to receiver distance or orientation of

This work was funded by the NSF under contract CNS-1618936 and CNS-1910655.

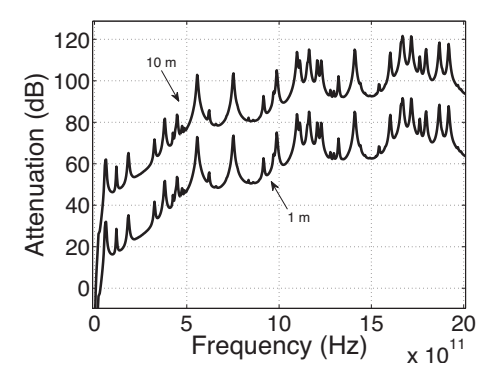


Fig. 1. Attenuation of terahertz for two distances.

the antenna arrays relative to one another or the presence of obstacles in the signal's path. These are all situations which will arise in any deployed terahertz system. In this paper we analyze a 2×2 MIMO system using measurement-driven emulation and study how small changes in relative antenna orientation will affect channel capacity. We use measurements at 140 GHz to obtain a MIMO channel matrix and then simulate the communication channel to evaluate performance.

A. Related Work

Traditional applications of terahertz have been in sensing. For example in detecting drugs, different types of explosives, detecting skin cancer and as a non-destructive way to do quality control for medication coatings, etc. [1], [2]. However, there is increasing interest in utilizing this frequency band for communications as well, due to the potential to provide very high data rates. A technological barrier to developing terahertz communications systems has been the difficulty in generating powerful enough terahertz transmissions. For instance, the microwave multiplier systems such as from [10] can provide milliwatts of power while the opto-electrical systems have output power of the order of micro watts only [11], [12]. However, things are beginning to change with more industries showing interest in exploiting this frequency band. For instance, Fujitsu recently demonstrated a compact 20 Gbps radio operating at 300 GHz [13].

Most research on terahertz communications has focussed on *fixed point-to-point links* utilizing simple modulation methods like OOK and PSK. For instance at the low-end of the terahertz

spectrum, Hirata et al [14] demonstrated 10 Gbps transmission at 120 GHz frequency over a distance of almost 6 km. Kallfass et al [15] demonstrated transmissions using OOK at 220 GHz and achieved 50 Gbps over 50 cm distances. Song et al [16] showed transmissions of 8 Gbps using ASK modulation over 250 GHz. Most recently, Jia et al [17] demonstrated 106 Gbps at 400 GHz using a photonic wireless link. There have been many other demonstrations as well [18]–[23] though a notable one was by Koenig et al [24] in which they achieved 100 Gbps over 20 m using a phased antenna array.

Our work looks at LoS MIMO links for terahertz. To date there has been only limited work in this domain. [3] was one of the earliest papers to consider terahertz MIMO for 5G. They conducted measurements in the 298-313 GHz band and provided estimates of capacity of a 2×2 system. However, they did not simulate a communication system. Rather, they rely on eye-charts to estimate capacity. They also do not consider relative offsets of antenna arrays.

B. Summary of Paper

The main results of the paper are that best performance is obtained when the inter-antenna spacing and the transmitter to receiver distance follows a specific relationship (equation 3). When the receiver antenna shifts with respect to the transmitter antenna or changes diustance, we see a sudden drop in performance as measured by BER versus Eb/No curves for uncoded QPSK.

The remainder of the paper is organized as follows. In the nect section we present the model for LoS MIMO links. The measurement setup is described in section 3, followed by the results in section 4. We conclude in section 5.

II. MODEL FOR MIMO LOS LINKS

Line-of-Sight (LoS) MIMO, first analyzed in [25], refers to the case where the non-line of sight paths between transmitter and receiver antennas is non-existent. This model has been studied for fixed microwave links and for mmWave as well [26]. For the purposes of our discussion, let us assume that both ends of a communication link have N antenna elements, numbered 1 to N. Let d_{ij} denote the distance between the ith element from one array to the jth element of the other array. Finally, let us assume that the two arrays are parallel to each other and the distance between them is D. Then, the channel response matrix \mathcal{H} for the LoS path can be written as [25], [27],

$$\mathcal{H} = \begin{pmatrix} e^{-jkd_{11}} & e^{-jkd_{12}} & \cdots & e^{-jkd_{1N}} \\ e^{-jkd_{21}} & e^{-jkd_{22}} & \cdots & e^{-jkd_{2N}} \\ \vdots & \vdots & \ddots & \vdots \\ \vdots & \vdots & \ddots & \vdots \\ e^{-jkd_{N1}} & e^{-jkd_{N2}} & \cdots & e^{-jkd_{NN}} \end{pmatrix}$$
(1)

where k is the wavenumber associated with the carrier frequency. The capacity of the channel is written as,

$$C = \log_2 \left(\det \left(\mathcal{I}_N + \frac{\rho}{N} \mathcal{H} \mathcal{H}^{\dagger} \right) \right) \text{ bps/Hz}$$
 (2)

where \mathcal{I}_N is the $N \times N$ identity and ρ is the SNR. The capacity is maximized when $\mathcal{H}\mathcal{H}^{\dagger} = N\mathcal{I}_N$. If we consider the case when the antenna elements are spaced uniformly with a distance of s between neighbors, then the maximum capacity is attained when,

 $s^2 = \frac{D\lambda}{N} \tag{3}$

Intuitively, what maximizing capacity above means is that the N channels are orthogonal to each other giving us the equivalent of N SISO (Single Input Single Output) channels that do not interfere with each other.

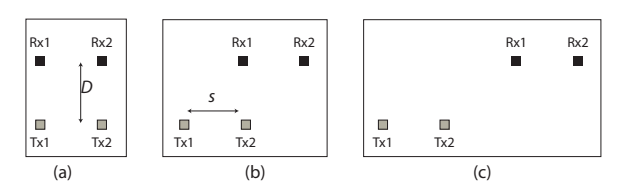


Fig. 2. Relative receiver offset.

In this paper we are considering a 2×2 system only but with non-optimal antenna placements. Specifically, we consider cases where the receiver antenna array is displaced laterally with respect to the transmit array as well as when it is at a different distance. Figure 2 illustrates these different cases. As shown in the figure, the inter-antenna spacing is fixed at s. We consider two different distances for D in our measurements. The displacement in Figure 2(b) is s and it is 2s in Figure 2(c). For any given placement of the antennas, we can write the channel capacity of a 2×2 MIMO system as.

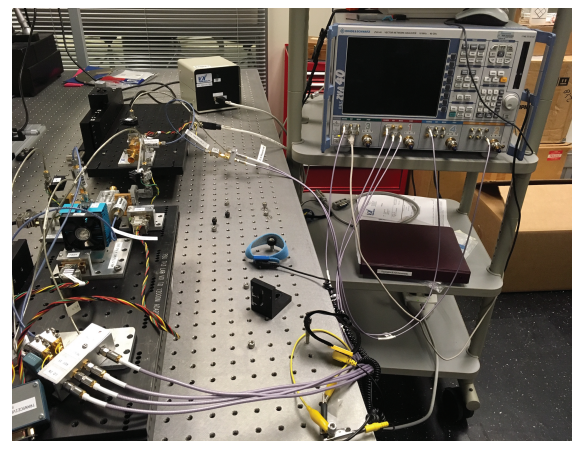
$$C = \log_2 \left((\rho + 1)^2 - \frac{\rho^2}{4} (2 + e^{jk(d_{11} + d_{22} - d_{21} - d_{12})} + e^{-jk(d_{11} + d_{22} - d_{21} - d_{12})} \right)$$
(4)

III. MEASUREMENT SETUP

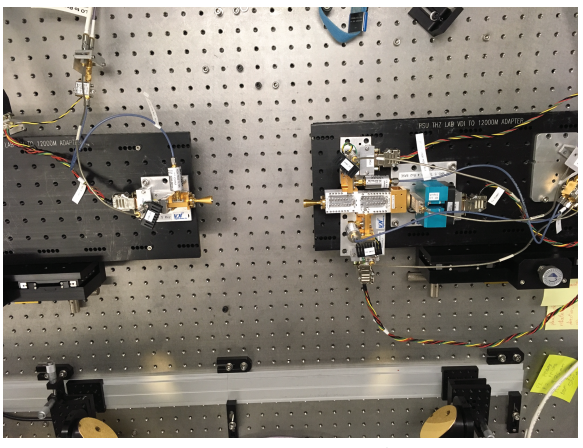
We use a Rhode & Schwartz Vector Network Analyzer (VNA) Figure 3(a). The setup is capable of producing signals up to 700 GHz. The transmit and receive antennas we use are horn antennas as shown in Figure 3(b) with gain 25 dBi and a 12⁰ half beam width (HBW). For this paper we only focus on the lower part of the terahertz spectrum – 115 to 165 GHz. This is one of the frequency windows that have lower atmospheric attenuation. Measurements were conducted in the lab where the ambient temperature was 72F and relative humidity was 40%. Other parameters of the experiment are given below:

Output power	5 dbm
Center Frequency	140 Ghz
Bandwidth	115 to 160 GHz
Number of points	1001
IF Bandwidth	1 kHz
Averaging	10

In order to ensure our measurement setup was correct, we first conducted a series of measurements where the transmit antenna is fixed and the receive antenna is placed in four



(a) Measurement System



(b) Top view of antennas

Fig. 3. Measurement setup.

different positions. Specifically, the distance between the transmit and receive arrays is fixed at 25cm. The measurements were conducted with the receive antenna then offset by 0cm, 1.64cm, 3.28cm, and 4.92cm. The downconverted magnitude response is shown in Figure 4. We plot the received phase at two antenna locations for a frequency of 140 GHz in Figure 5. Simple calculations show that the relative phase change is consistent with the lateral antenna displacement. Finally, we plot the relative attenuation when the receiver moves from 12.5cm to 25cm and when it moves from 25cm to 50cm, Figure 6. The notable feature here is that signal strength drops rapidly with distance (as observed in Figure 1) with the implication that any terahertz channel will degrade rapidly with increasing distance, unless we compensate with higher transmit power or antenna gain or spatial techniques such as MIMO.

IV. Results of 2×2 LoS MIMO Communication Channel with Offset

We next study how change in distance and relative offset of the receiver will affect the communication channel. We assume that the data stream is divided into two independent streams

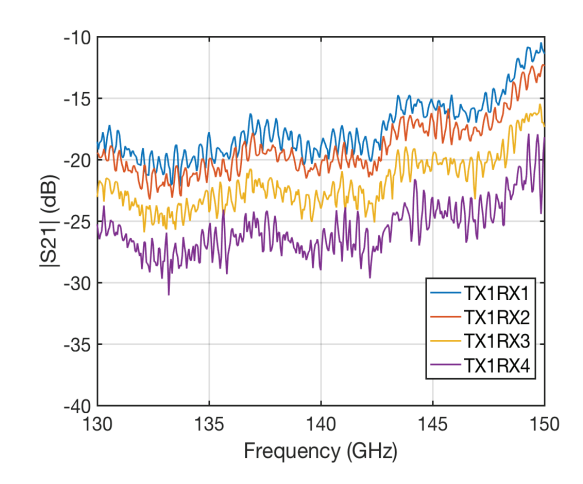


Fig. 4. Magnitude of TX1 at four offset RX locations.

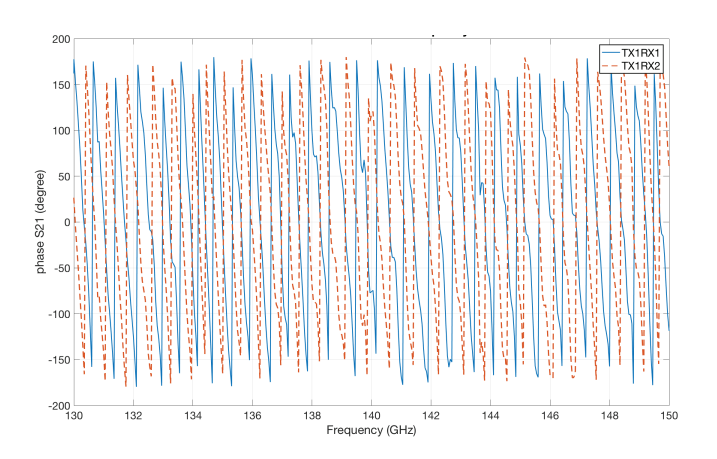


Fig. 5. Signal phase at two offset receiver positions.

and each is modulated using QPSK. This provides us with a multiplexing gain and we do not require explicit space-time coding. For the receiver, we assume perfect channel estimation and optimal Maximum-Likelihood Estimation. Thus, our results provide an upper bound on the best achievable channel performance. We utilize the channel measurements to create the channel matrix $\mathcal H$ for each case and then run simulations using this matrix.

We divided our study into two parts. The first part focuses on how receiver antenna offset relative to the sender will affect performance. The assumption made here is that the inter-antenna spacing s is optimal for when the transmit and receive antennas are perfectly aligned. We consider two Tr/Rx distances $D=12.5 \, \mathrm{cm}$ and $50 \, \mathrm{cm}$ with inter-antenna spacing of $1.16 \, \mathrm{cm}$ and $2.31 \, \mathrm{cm}$ respectively. For each case, we consider offsets of s and 2s. Figures 7 and 8 plot the BER versus Eb/No for these cases.

We first observe that for both distances D, an increase in offset results in worsening performance. This is because as the offset increases, there is a loss of independence between the spatial channels and \mathcal{HH}^{\dagger} is no longer close to $N\mathcal{I}_N$.

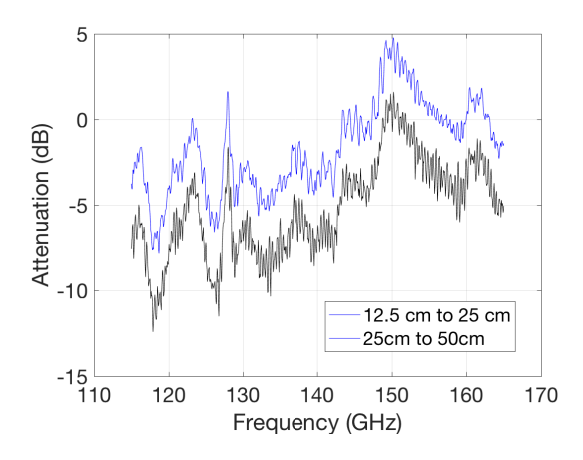


Fig. 6. Relative drop in magnitude with distance.

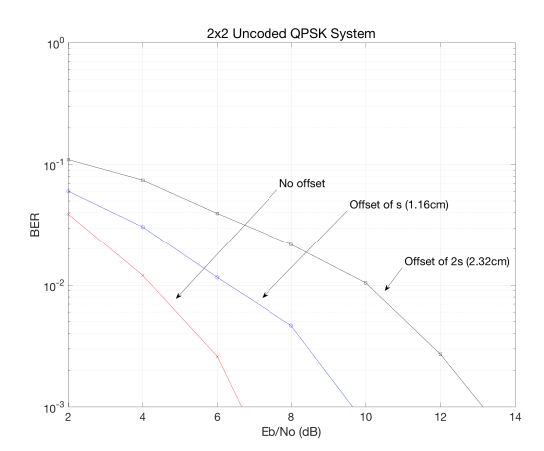


Fig. 7. ML Receiver performance $D=12.5\mathrm{cm}$ and $s=1.16\mathrm{cm}$ (optimal).

Comparing the two figures, however, we note something counter-intuitive. We see that with the exception of the no offset case, the curves are skewed towards higher Eb/No values for the shorter distance of 12.5cm (for the same BER). To understand this, note that in the no offset case we have a better channel at a smaller distance because the horn antenna has a very narrow beam which results in a much stronger signal at 12.5cm as compared to 50cm distance. For the offset cases, the reason the 50cm distance shows better performance relative to the 12.5cm distance is because the offset angle at an offset of s is 84.69^{0} for 12.5 while it is 87.35^{0} for 50cm (the no offset case corresponds to an angle of 90°). Similarly, for an offset of 2s the angles are, respectively, 79.48^{0} and 84.72^{0} . Having a narrower angle for the longer distance means that the channel is closer to optimal (zero offset) and hence we see better performance for the longer distance.

For the second study, we fix the inter-antenna spacing at the transmitter and receiver to $s=1.16\mathrm{cm}$ (i.e., the optimal value for $D=12.5\mathrm{cm}$). However, we then move the receiver antenna to a distance of 50cm and look at the zero offset, $s=1.16\mathrm{cm}$ and $2s=2.32\mathrm{cm}$ offset cases. This is a more realistic situation because in any real-life scenario the antenna

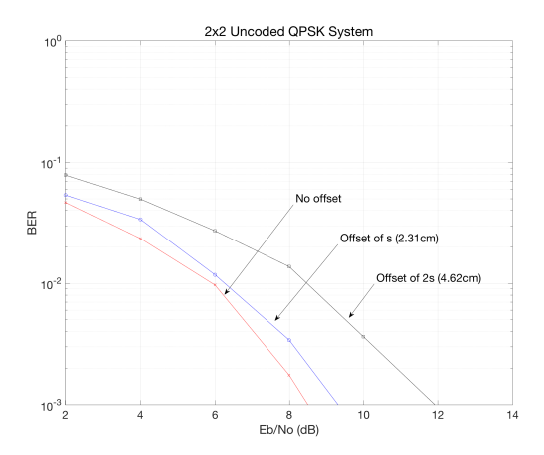


Fig. 8. ML Receiver performance D = 50cm and s = 2.31cm (optimal).

spacing at a device is fixed. We plot the BER versus Eb/No curves for the 50cm distance in Figure 9.

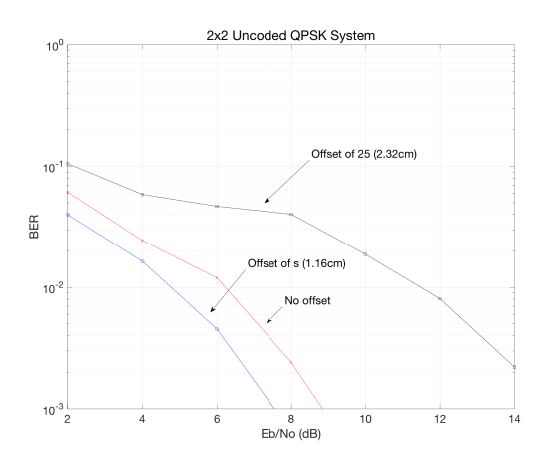


Fig. 9. D = 50cm, s = 12.5cm.

Let us first compare the no offset case between Figure 9 and 8. The performance is somewhat degraded when the value of s is 1.16cm since that is not the optimal antenna separation for 50cm distance. However, we note that when the offset is 1.16cm in Figure 9 the performance is better than the no offset case. Examining the various d_{ij} values, it turns out that this is a very special case that results in better channel separation at the receiver due to the offset. Finally, as the offset is increased even further to 2.32cm the performance degrades rapidly. This is expected since the channels are highly correlated.

V. CONCLUSIONS

In this paper we study a novel MIMO problem that will arrise in terahertz systems. Given the small wavelengths at these frequencies, the optimal antenna separation in an array is small. As a result, any movement by the transmitter or receiver can very quickly make the channel poor. Though, in some rare case as illustrated by the offset of *s* case in Figure 9, the performance suddenly improves. This suggests that

terahertz MIMO may be better suited to static deployments rather than mobile deployments. Alternatively, it may be a better strategy to utilize antenna arrays to create smart antenna systems to boost gain and mitigate the huge attenuation. Future work will expand the measurements for 2×2 MIMO systems to more distances and offsets. This will give us a better understanding of how rapidly the channel can degrade as a function of variable distances and offsets. We will also conduct measurement studies of non-parallel antenna arrays.

REFERENCES

- J. F. Federici, D. Gary, R. Barat, and D. Zimdars, "THz standoff detection and imaging of explosives and weapons," in *Defense and Security*. International Society for Optics and Photonics, 2005, pp. 75–84.
- [2] D. Woolard, P. Zhao, C. Rutherglen, Z. Yu, P. Burke, S. Brueck, and A. Stintz, "Nanoscale imaging technology for THz-frequency transmission microscopy," *International Journal of High Speed Electronics and Systems*, vol. 18, no. 01, pp. 205–222, 2008.
- [3] N. Khalid and O. B. Akan, "Experimental throughput analysis of low-thz mimo communication channel in 5g wireless networks," *IEEE Wireless Communication Letters*, vol. 5, no. 6, pp. 616–619, December 2016.
- [4] F. Moshir and S. Singh, "Modulation for indoor terahertz communication networks," in *Journal of Nano Communication Networks*, Elsevier (Special Issue on Terahertz Communications), 2016.
- [5] I. Kallfass, F. Boes, T. Messinger, J. Antes, U. Inam, A. Lewark, and R. Tessman, "64 gbit/s transmission over 850 m fixed wireless link at 240 ghz carrier frequency," *Journal of Infrared, millimeter, and terahertz* waves, vol. 36, pp. 221–233, January 2015.
- [6] I. Akyildiz, J. M. Jornet, and C. Han, "Teranets: ultra-broadband communication networks in the terahertz band," *IEEE Wireless Communications*, vol. 21, no. 4, pp. 130–135, 2014.
- [7] T. Kleine-Ostmann and T. Nagatsuma, "A review on terahertz communications research," *Journal of Infrared, Millimeter, and Terahertz Waves*, vol. 32, no. 2, pp. 143–171, 2011.
- [8] "Ieee 802.15 wpan terahertz interest group (igthz)," www.ieee802.org/15/pub/IGthzOLD.html, November 12 2015.
- [9] "Itu-r: Future technology trends of terrestial imt systems," Report ITU-R M.2320-0. November 2014.
- [10] "Virginia diodes," http://www.vadiodes.com.
- [11] M. Exter, C. Fattinger, and D. Grischkowsky, "Terahertz time-domain spectroscopy of water vapor," *Optic Letters*, vol. 14, no. 20, pp. 1128– 1130, 1989
- [12] D. Huang, T. R. LaRocca, M.-C. Chang, L. Samoska, A. Fung, R. L. Campbell, and M. Andrews, "Terahertz CMOS frequency generator using linear superposition technique," *IEEE Journal of Solid-State Circuits*, vol. 43, no. 12, pp. 2730–2738, 2008.
- [13] Y. Nakasha, S. Shiba, Y. Kawano, and T. Takahashi, "Compact terahertz receiver for short-range wireless communications of tens of gbps," *Fujitsu Science and Technology Journal*, vol. 53, no. 2, pp. 9–14, Feburary 2017.
- [14] A. Hirata, T. Kosugi, H. Takahashi, J. Takeuchi, K. Murata, N. Kukutsu, Y. Kado, S. Okabe, T. Ikeda, F. Suginosita et al., "5.8-km 10-Gbps data transmission over a 120-GHz-band wireless link," in 2010 IEEE International Conference on Wireless Information Technology and Systems (ICWITS). IEEE, 2010, pp. 1–4.
- [15] I. Kallfass, J. Antes, T. Schneider, F. Kurz, D. Lopez-Diaz, S. Diebold, H. Massler, A. Leuther, and A. Tessmann, "All active MMIC-based wireless communication at 220 GHz," *IEEE Transactions on Terahertz Science and Technology*, vol. 1, no. 2, pp. 477–487, November 2011.
- [16] H. Song, K. Ajito, A. Hirata, A. Wakatsuki, T. Furuta, N. Kukutsu, and T. Nagatsuma, "Multi-gigabit wireless data transmission at over 200-GHz," in 34th International Conference on Infrared, Millimeter, and Terahertz Waves, 2009. IRMMW-THz 2009, 2009, pp. 1–2.
- [17] S. Jia, X. Pang, O. Ozolins, X. Yu, H. Hu, J. Yu, P. Guan, F. D. Ros, S. Popov, G. Jacobsen, M. Galili, T. Morioka, D. Zibar, and L. K. Oxenlowe, "0.4 thz photonic-wireless link with 106 gb/s single channel bitrate," *Journal of Lightwave Technology*, vol. 36, no. 2, pp. 610–616, January 2018.

- [18] J. Antes, J. Reichart, D. Lopez-Diaz, A. Tessmann, F. Poprawa, F. Kurz, T. Schneider, H. Massler, and I. Kallfass, "System concept and implementation of a mmW wireless link providing data rates up to 25 Gbit/s," in 2011 IEEE International Conference on Microwaves, Communications, Antennas and Electronics Systems (COMCAS), Nov 2011, pp. 1–4.
- [19] B. Zhang, Y.-Z. Xiong, L. Wang, and S. Hu, "A switch-based ASK modulator for 10 Gbps 135 GHz communication by 0.13 MOSFET," *IEEE Microwave and Wireless Components Letters*, vol. 22, no. 8, pp. 415–417, 2012.
- [20] H. Song, K. Ajito, Y. Muramoto, and A. Wakatasuki, "24 Gbit/s data transmission in 300 GHz band for future terahertz communications," *Electronics Letters*, vol. 48, no. 15, pp. 953–954, July 2012.
- [21] G. Ducournau, P. Szriftgiser, A. Beck, D. Bacquet, F. Pavanello, E. Peytavit, M. Zaknoune, T. Akalin, and J.-F. Lampin, "Ultrawide-bandwidth single-channel 0.4-THz wireless link combining broadband quasi-optic photomixer and coherent detection," 2014.
- [22] C. Wang, C. Lin, Q. Chen, B. Lu, X. Deng, and J. Zhang, "A 10-Gbit/s wireless communication link using 16-QAM modulation in 140-GHz band," *IEEE Transactions on Microwave Theory and Techniques*, vol. 61, no. 7, pp. 2737–2746, July 2013.
- [23] B. Lu, W. Huang, C. Lin, and C. Wang, "A 16QAM modulation based 3Gbps wireless communication demonstration system at 0.34 THz band," in *Infrared, Millimeter, and Terahertz Waves (IRMMW-THz)*, 2013 38th International Conference on. IEEE, 2013, pp. 1–2.
- [24] S. Koenig, D. Lopez-Diaz, J. Antes, F. Boes, R. Henneberger, A. Leuther, A. Tessmann, R. Schmogrow, D. Hillerkuss, R. Palmer, T. Zwick, C. Koos, W. Freude, O. Ambacher, J. Leuthold, and I. Kallfass, "Wireless sub-THz communication system with high data rate," *Nature Photonics*, vol. 7, pp. 977–981, October 2013.
- [25] D. Gesbert, H. Bolcskei, D. Gore, and A. Paulraj, "Outdoor mimo wireless channels: models and performance prediction," *IEEE Transactions* on Communications, vol. 50, no. 12, pp. 1926–1934, December 2002.
- [26] C. Sheldon, E. Torkildson, M. Seo, C. P. Yue, M. Rodwell, and U. Madhow, "Spatial multiplexing over a line-of-sight millimeter-wave mimo link: two-channel hardware demonstration at 1.2gbps over 41m range," in *European Conference on Wireless Technology*, 27-28 October 2008, pp. 198–201.
- [27] I. Sarris and A. R. Nix, "Maximum mimo capacity in line-of-sight," in *International Conference on Information Communications and Signal Processing*, Bankok, Thailand, 6-9 December 2005.